Theory of a Cooled Spherical Electrostatic Probe in a Continuum Gas

ROBERT L. CHAPKIS* AND ERIC BAUM†
TRW Systems Group, Redondo Beach, Calif.

The idealized problem of a cooled spherical electrostatic probe in a quiescent continuum slightly ionized chemically frozen gas has been investigated. The electron temperature is described by two limiting models; either the electrons are assumed to be at local thermal equilibrium, or they are assumed frozen at the ambient temperature far from the probe. From numerical solutions of the governing equations, it has been found that with the frozen electron temperature assumption, the probe characteristics for a cold probe are only slightly altered from those of an adiabatic probe. With the electrons at thermal equilibrium, the probe characteristic is only slightly altered when the bias potential is large, but significant changes in the probe characteristic do occur when the bias potential is small, including a significant shift in the floating potential.

Nomenclature

$C_{\pm}$ = charged particle mass fraction
$D_{\pm}$ = diffusion coefficient of a charged particle in the neutral gas
$\bar{D}_{\pm}$ = $D_{\pm}/D_{\pm\infty}$
e = absolute value of the charge on a charged particle
E^* = dimensionless electric field = $-(e\lambda_0/kT_{-\infty})d\phi/dr$
$J_{\pm}$ = normalized charged particle flux = $-(\Gamma_{\pm}r)_p/D_{\pm\infty}N_{\infty}$
J_T = dimensionless net charge flux = $-(\Gamma_{+p} - \Gamma_{-p})e^2r_p{}^3/\epsilon_0T_{-\infty}D_{+\infty}$
k = Boltzmann constant
K = J_-/J_+
$M_{\pm}$ = charged particle molecular weight
$N_{\pm}$ = charged particle number density
r = radial distance measured from center of probe
$r_p{}^*$ = dimensionless probe radius = r_p/λ_0
s = normalized distance from probe = $(r - r_p)/\lambda_0$
T = temperature
$\bar{T}$ = temperature ratio = T/T_{∞}
α = ratio of diffusion coefficients = D_+/D_-
$\beta_{\pm}$ = normalized charged particle concentration = $(C_{\pm}/C_{\pm\infty})(\lambda_0/\lambda_D)^2$
$\bar{\beta}$ = $(\beta_+ + \beta_-)/2$
$\Gamma_{\pm}$ = flux density of charged particles
δ = $(\beta_+ - \beta_-)/2$
ϵ_0 = permittivity of empty space
ζ = r_p/r
κ = thermal conductivity
λ_D = reference Debye length = $(\epsilon_0kT_{-\infty}/N_{\infty}e^2)^{1/2}$
λ_0 = characteristic length = $[r_p\lambda_D{}^2/J_+(1 + K)]^{1/3}$
ρ = gas density
$\rho_p{}^2$ = dimensionless charged species concentration = $(r_p/\lambda_D)^2 = N_{\infty}e^2r_p{}^2/\epsilon_0kT_{-\infty}$
τ = $T_{+\infty}/T_{-\infty}$
ϕ = electrostatic potential
$\phi_p{}^*$ = dimensionless probe potential = $e\phi_p/kT_{-\infty}$

Subscripts

$+$ = positively charged particle
$-$ = negatively charged particle
p = conditions evaluated at the probe surface
∞ = conditions evaluated at $r \to \infty$

Received January 11, 1971, revision received May 10, 1971. The authors wish to acknowledge the assistance of Michael A. Bilyk, who wrote the computer program used to obtain the data presented in this paper.
Index category: Plasma Dynamics and MHD.

* Staff Engineer, Re-entry Physics Department; now Senior Engineer, Tetra Tech, Inc., Pasadena, Calif. Associate Fellow AIAA.
† Staff Engineer, Fluid Mechanics Laboratory. Member AIAA.

1. Introduction

ELECTROSTATIC probes have proved to be extremely useful tools for the experimental investigation of plasma properties. However, in order to interpret the measurements made by the probes, it is necessary to have, first, a realistic theoretical model with which to relate measured electrical currents and voltages to such plasma properties as charged particle number density. A number of investigators have studied an idealized model of a spherical electrostatic probe for use in the regime where the continuum assumption is appropriate. In addition to the continuum approximation, these investigators make several other assumptions about the state of the plasma, namely that 1) the plasma is but slightly ionized, 2) properties are spherically symmetric, 3) the probe surface is catalytic, 4) the Einstein relation between mobility and diffusivity holds, and 5) the temperature of the gas surrounding the probe is uniform.

Both approximate[1-3] and exact numerical[4,5] solutions of the equations describing this idealized model have been obtained and these solutions have proved useful in interpreting probe measurements. However, for many cases the temperature of the probe is much colder than the temperature of the surrounding gas and, therefore, a nonuniform temperature field exists about the probe. Since the charged particle diffusion coefficients and the local gas density are temperature dependent, one might expect that the characteristics of the probe would be significantly changed by the nonuniform temperature field. The only previous attempt to determine the magnitude of this effect is one made by Thomas[6] for the case of a highly negative probe. Thomas' analysis was similar to that of Su and Lam[2] for the constant temperature case, and he assumed that the ion temperature was determined by the heat conduction equation and that the electron temperature was "frozen." Unfortunately, he used an incompressible form of the diffusion flux expressions that does not completely account for the effect of gas density gradient on probe current. His results showed only a slight effect of nonuniform temperature on the probe current-voltage characteristic for the highly negative probe.

It might be expected, however, that the effects of nonuniform temperature would be more important at lower probe potentials and for cases where there are enough collisions within the sheath to bring the electrons (or heavy negative ions) close to local thermal equilibrium. In order to determine whether or not this is so, computations have been made to obtain the exact numerical solutions of the governing probe equations. These solutions cover a wide range of probe potential and ratio of probe radius to Debye length, and consider two limiting cases for the negative particle temperature description; at local thermal equilibrium, or frozen at the temperature of the ambient gas infinitely far from the probe.

2. Equations

The basic equations governing the charged particle distribution and the potential field about the probe are the two continuity equations for the positive and negative particles, Poisson's equation relating the potential to the charged particle distribution, and the heat conduction equation that determines the temperature distribution in the surrounding gas. For spherical symmetry these are:

$$\begin{aligned}(d/dr)(r^2\Gamma_+) &= 0\\ (d/dr)(r^2\Gamma_-) &= 0\\ (1/r^2)(d/dr)[r^2(d\phi/dr)] &= (-\rho e/\epsilon_0)(C_+/M_+ - C_-/M_-)\\ (d/dr)[\kappa r^2(dT/dr)] &= 0\end{aligned} \quad (1)$$

The flux densities are related to the gradients of charged particle density and potential and to the temperature by the following equation:

$$\Gamma_\pm = (\rho D_\pm/M_\pm)[-dC_\pm/dr \mp (e/kT_\pm)C_\pm(d\phi/dr)] \quad (2)$$

Thermal diffusion (driven by gradients in T, T_+ and T_-) has been neglected and we have assumed that the Einstein relation between the diffusion coefficients and the mobilities holds. The temperature dependence of the diffusion coefficients is generally quite complex for a real gas, so for the purposes of the present calculations, we will postulate a rigid sphere model gas. That is, we take $D_\pm \propto \bar{v}_\pm\lambda$, where $\bar{v}_\pm$ is the mean particle velocity of the positive or negative particles, and λ is the mean free path of the charged particle in neutral ambient gas. Since the mean free path is proportional to the temperature T, and the mean particle velocity is proportional to the square root of the charged-particle temperature, we obtain the following relation for the temperature dependence of the diffusion coefficients:

$$D_\pm \propto T_\pm^{1/2}T \quad (3)$$

In what follows we shall consider two separate cases. In the first, both the positive and negative particle are in thermal equilibrium with the local ambient gas in which case $T_\pm = T$ and $D_\pm \propto T^{3/2}$. In the second case the positive particles are in thermal equilibrium with the local ambient gas, but the negative particles have a constant mean temperature. In that case $T_+ = T$, $T_- = \text{constant} = T_{-\infty}$, $D_+ \propto T^{3/2}$, and $D_- \propto T$.

For either case, the first two of Eq. (1) can be integrated and the results combined with Eq. (2) to yield the following:

$$(D_+\rho r^2/D_{+\infty}r_pM_+N_\infty)[-dC_+/dr - (e/kT_+)C_+(d\phi/dr)] = -J_+ \quad (4)$$

$$(D_-\rho r^2/D_{-\infty}r_pM_-N_\infty)[-dC_-/dr + (e/kT_-)C_-(d\phi/dr)] = -J_- \quad (5)$$

where N_∞ is the number density of positive or negative particles at $r \to \infty$, and the unknown constants $J_\pm$ are the normalized particle fluxes received by the probe, i.e., $N_\infty = (\rho C_+)_\infty/M_+ = (\rho C_-)_\infty/M_-$, $J_\pm = -(\Gamma_\pm r)_p/D_{\pm\infty}N_\infty$. The normalization is such that $J_\pm = 1$ for the adiabatic probe at plasma potential.

At the probe surface $r = r_p$; $C_+ = C_- = 0$, $\phi = \phi_p$, $T = T_p$. In the undisturbed plasma $r \to \infty$; $C_+ = N_\infty M_+/\rho_\infty$, $C_- = N_\infty M_-/\rho_\infty$, $\phi = 0$, $T = T_\infty$.

In order to put the equations into a form convenient for numerical integration, we first define two characteristic lengths λ_D = Debye length = $[\epsilon_0 kT_{-\infty}/N_\infty e^2]^{1/2}$, and $\lambda_0 = [r_p\epsilon_0 kT_-/J_+(1 + K)N_\infty e^2]^{1/3} = [r_p\lambda_D^2/J_+(1 + K)]^{1/3}$ where $K = J_-/J_+$.

We also define the following dimensionless dependent and independent variables: $E^* = -(e\lambda_0/kT_{-\infty})d\phi/dr$, $\beta_\pm = (C_\pm/C_{\pm\infty})(\lambda_0/\lambda_D)^2$, $s = (r - r_p)/\lambda_0$.

The equations and boundary conditions then become

$$dE^*/ds + 2E^*/(r_p^* + s) = (\beta_+ - \beta_-)/\bar{T}_+ \quad (6a)$$

$$1/(1 + K) = (\bar{D}_+/\bar{T}_+)(1 + s/r_p^*)^2[d\beta_+/ds - (1/\tau\bar{T}_+)\beta_+E^*] \quad (6b)$$

$$K/(1 + K) = (\bar{D}_-/\bar{T}_+)(1 + s/r_p^*)^2[d\beta_-/ds + (1/\bar{T}_-)\beta_-E^*] \quad (6c)$$

$$E^*(0) = E_p^*,\ \beta_+(0) = \beta_-(0) = 0$$

where $r_p^* = r_p/\lambda_0$, $\bar{D}_\pm = D_\pm/D_{\pm\infty}$, $\bar{T}_\pm = T_\pm/T_{\pm\infty}$, and $\tau = T_{+\infty}/T_{-\infty}$. E_p^* is the particular value of $E^*(0)$ for which the boundary condition at $s \to \infty(\beta_- \to \beta_+)$ is satisfied. The parameter K is a monotonic function of the probe potential, which can be determined a posteriori by integration

$$\phi_p^* = \frac{e\phi}{kT_{-\infty}} = \int_0^\infty E^* ds$$

Before Eq. (6) can be solved, however, the temperature distribution must first be determined from the last of Eqs. (1). The solution for the nondimensional temperature $\bar{T} = T/T_\infty$ is

$$\bar{T} = [1 + (\bar{T}_p^{1+\omega} - 1)/(1 + s/r_p^*)]^{1/1+\omega} \quad (7)$$

where the thermal conductivity κ has been assumed to be proportional to the ω power of temperature. Taking $\omega = \frac{1}{2}$, the corresponding expression for the normalized diffusion coefficient of the positive particles is $\bar{D}_+ = \bar{T}^{3/2}$ where

$$\bar{T} = [1 + (\bar{T}_p^{3/2} - 1)/(1 + s/r_p^*)]^{2/3} \quad (8)$$

As mentioned previously, the diffusion coefficient for the negatively charged particles depends on whether or not they are in thermal equilibrium with the ambient gas; if so then $\bar{D}_- = \bar{D}_+ = \bar{T}^{3/2}$. On the other hand, if the temperature of the electrons is "frozen" then $\bar{D}_- = \bar{T}$.

3. Saturation Currents

In the limit $r_p^* \to \infty$ the sheath becomes negligibly thin compared to the probe radius. Since the sheath remains negligibly thin under any imposed finite bias potential, the flux of a charged species to the probe is limited by the ambipolar flux towards the probe outside of the sheath. Combining Eqs. (4) and (5) to eliminate the field, the following expression for the ambipolar charged particle concentrations is obtained:

$$\begin{aligned}&d/d(r/r_p)\{(T_\infty/T)(r/r_p)^2[(T_+/T_\infty) + (T_-/T_\infty)]d(C/C_\infty)/d(r/r_p)\} = \\ &J_+ d/d(r/r_p)[(T_+/T_\infty)/(D_+/D_{+\infty})] + J_- d/d(r/r_p)[(T_-/T_\infty)/(D_-/D_{-\infty})] \quad (9)\end{aligned}$$

$$C/C_\infty(\infty) = 1,\ C/C_\infty(1) = 0$$

It is interesting to note here that the ambipolar concentrations are independent of the positive and negative particle dimensionless probe currents (J_+,J_-) only when T_+/D_+ and T_-/D_- are both constant. The cases of current interest have $T/T_\infty = T_+/T_\infty = (1 - br_p/r)^{2/3}$ where $b = 1 - (T_p/T_\infty)^{3/2}$, $D_+/D_{+\infty} = (T/T_\infty)^{3/2}$. Depending on the sign of the probe bias and the electron temperature assumption, we then find that:

Case I: $T_-/T_\infty = 1$, $D_-/D_{-\infty} = T/T_\infty$ (frozen electron temperature)

$$J_- = 0 \text{ (ion collection saturation)}$$

$$C = \frac{3}{2}\frac{J_+}{b}\left[\frac{T}{T_\infty} - \frac{T_p}{T_\infty} - \ln\left(\frac{1+T/T_\infty}{1+T_p/T_\infty}\right)\right]$$

$$J_+ = \frac{2}{3}b\bigg/\left[1 - \frac{T_p}{T_\infty} + \ln\left(\frac{1+T_p/T_\infty}{2}\right)\right] \tag{10}$$

Case II: frozen electron temperature

$$J_+ = 0 \text{ (electron collection saturation)}$$

$$C = \frac{3J_-}{b}\left[\left(\frac{T}{T_\infty}\right)^{1/2} - \left(\frac{T_p}{T_\infty}\right)^{1/2} - \tan^{-1}\left(\frac{T}{T_\infty}\right)^{1/2} + \tan^{-1}\left(\frac{T_p}{T_\infty}\right)^{1/2}\right]$$

$$J_- = \frac{b}{3\left[1 - \left(\frac{T_p}{T_\infty}\right)^{1/2} - \frac{\pi}{4} + \tan^{-1}\left(\frac{T_p}{T_\infty}\right)^{1/2}\right]} \tag{11}$$

Case III: $T_-/T_\infty = T/T_\infty$, $D_-/D_{-\infty} = (T/T_\infty)^{3/2}$ (equilibrium electron temperature)

$$J_- = 0 \text{ (ion collection saturation)}$$

or

$$J_+ = 0 \text{ (electron collection saturation)}$$

$$C = (3J_\pm/4b)[(T/T_\infty) - (T_p/T_\infty)]$$

$$J_\pm = 4b/3(1 - T_p/T_\infty) \tag{12}$$

It can be seen that the isothermal limit for these cases ($b \to 0$) is the expected $J_\pm \to 2$.

4. "Point-Probe" Solution

An interesting limiting case for which a simple closed-form solution can be obtained is the case where the ratio ϵ of probe radius to Debye length shrinks to zero. In order to obtain that solution, it is convenient to write Eqs. (1) in a different form than that appropriate for numerical solution. Thus we shall use as the independent variable $\zeta = r_p/r$, and as dependent variables $\bar{C}_\pm = C_\pm/C_{\pm\infty}$ and $\phi^* = e\phi/kT_-$. The equations and boundary conditions in these variables are the following:

$$\zeta^4 d^2\phi^*/d\zeta^2 = \bar{p}\epsilon^2(\bar{C}_+ - \bar{C}_-)$$

$$d\bar{C}_+/d\zeta + (\bar{C}_+/\tau\bar{T}_+)d\phi^*/d\zeta = -J_+/\bar{p}\bar{D}_+$$

$$d\bar{C}_-/d\zeta - (\bar{C}_-/\bar{T}_-)d\phi^*/d\zeta = -J_-/\bar{p}\bar{D}_-$$

$$\text{At } \zeta = 0;\ \phi^* = 0,\ \bar{C}_+ = \bar{C}_- = 1$$

$$\text{At } \zeta = 1;\ \phi^* = \phi_p^*,\ \bar{C}_+ = \bar{C}_- = 0 \tag{13}$$

In order to obtain the limiting solution for $\epsilon \to 0$ we expand ϕ^*, $\bar{C}_\pm$, and $J_\pm$ as follows:

$$\phi^*(\zeta;\epsilon,\phi_p^*) = \phi_1^*(\zeta;\phi_p^*) + \ldots$$

$$C_\pm(\zeta;\epsilon,\phi_p^*) = C_{\pm1}(\zeta;\phi_p^*) + \ldots \tag{14}$$

$$J_\pm(\epsilon,\phi_p^*) = J_{\pm1}(\phi_p^*) + \ldots$$

After substituting these expansions into Eqs. (13) and letting $\epsilon \to 0$, we obtain the following equations for ϕ_1^*, $\bar{C}_{\pm1}$, and $J_{\pm1}$:

$$\zeta^4 d^2\phi_1^*/d\zeta^2 = 0$$

$$d\bar{C}_{-1}/d\zeta - (\bar{C}_{-1}/\bar{T}_-)d\phi_1^*/d\zeta = -J_{-1}/\bar{p}\bar{D}_- \tag{15}$$

$$d\bar{C}_{+1}/d\zeta + (\bar{C}_{+1}/\tau T_+)d\phi_1^*/d\zeta = -J_{+1}/\bar{p}\bar{D}_+$$

The solution of Eqs. (15) that satisfies the boundary conditions at $\zeta = 1$ is the following:

$$\phi_1^* = \phi_p^*\zeta$$

$$\bar{C}_{-1} = -J_{-1}\left\{\exp\left[-\phi_p^*\int^\zeta (1/\bar{T}_-)d\zeta\right]\right\} \times \int_1^\zeta (1/\bar{p}\bar{D}_-)\exp\left[\phi_p^*\int^\zeta (1/\bar{T}_-)d\zeta\right]d\zeta \tag{16}$$

$$\bar{C}_{+1} = -J_{+1}\left\{\exp\left[(\phi_p^*/\tau)\int^\zeta (1/\bar{T}_+)d\zeta\right]\right\} \int_1^\zeta (1/\bar{p}\bar{D}_+)\exp\left[-(\phi_p^*/\tau)\int^\zeta (1/\bar{T}_+)d\zeta\right]d\zeta$$

The solution given by Eqs. (16) holds for any temperature distribution or for any form of the diffusion coefficients. Thus for the positive particle temperature given by Eq. (8), i.e., $\bar{T}_+ = (1 - b\zeta)^{2/3}$ where $b = 1 - \bar{T}_p^{3/2}$ and for $\bar{D}_+ = \bar{T}_+^{3/2}$ we obtain from Eqs. (16)

$$\bar{C}_{+1} = -(b\tau/3\phi_p^*)(\tau/\phi_p^*)J_{+1}\{[(3\phi_p^*/b\tau)(1-b)^{1/3} - 1] \times \exp[-(3\phi_p^*/b\tau)((1-b\zeta)^{1/3} - (1-b)^{1/3})] - [(3\phi_p^*/b\tau)(1-b\zeta)^{1/3} - 1]\} \tag{17}$$

For the case where $\bar{T}_- = \bar{T}_+$ we also obtain

$$\bar{C}_{-1} = +(b/3\phi_p^*)(1/\phi_p^*)J_{-1}\{[(3\phi_p^*/b)(1-b)^{1/3} + 1] \times \exp[(3\phi_p^*/b)((1-b\zeta)^{1/3} - (1-b)^{1/3})] - [(3\phi_p^*/b)(1-b\zeta)^{1/3} + 1]\} \tag{18}$$

whereas for the case of $\bar{T}_- = 1$ we obtain

$$\bar{C}_{-1} = (J_{-1}/\phi_p^*)\{\exp[(1-\zeta)\phi_p^*] - 1\} \tag{19}$$

In order to obtain explicit relations for J_{+1} and J_{-1} in terms of the probe potential and temperature we evaluate Eqs. (17–19) at $\zeta = 0$‡ and solve for J_{+1} and J_{-1}. For J_{+1} we obtain the following:

$$J_{+1} = (3\phi_p^*/b\tau)(\phi_p^*/\tau)/\big([(3\phi_p^*/b\tau) - 1] - [(3\phi_p^*/b\tau)(1-b)^{1/3} - 1]\exp\{(-3\phi_p^*/b\tau)[1 - (1-b)^{1/3}]\}\big) \tag{20}$$

For J_{-1} we obtain for the case of $\bar{T}_- = \bar{T}_+$

$$J_{-1} = (3\phi_p^*/b)\phi_p^*/\big([(3\phi_p^*/b)(1-b)^{1/3} + 1] \times \exp\{(3\phi_p^*/b)[1 - (1-b)^{1/3}]\} - [(3\phi_p^*/b) + 1]\big) \tag{21}$$

whereas for the case of $\bar{T}_- = 1$ we obtain

$$J_{-1} = \phi_p^*/(\exp\phi_p^* - 1) \tag{22}$$

and, thus, for that case we find that J_{-1} is independent of the probe temperature. We also find from Eq. (20) that for the probe potential ϕ_p^* approaching infinity, $J_{+1} \sim \phi_p^*/\tau$. Thus, for large potential J_{+1} also becomes independent of the probe temperature. On the other hand, for $\phi_p^* = 0$ we find from Eq. (20) that $J_{+1} = (2b/3)/[1 - (1-b)^{2/3}]$, and therefore for the limiting case of zero probe-temperature; i.e., $b = 1$, $J_{+1} = \frac{2}{3}$ for $\phi_p^* = 0$, compared with a value of $J_{+1} = 1$ for the uniform temperature case.

5. Asymptotic Behavior for $s \to \infty$

In order to obtain numerical solutions to Eqs. (6) it is first necessary to determine the asymptotic behavior of β_+, β_-, and E^* as $s \to \infty$. To illustrate how the asymptotic solution

‡ The lowest-order expressions for $\bar{C}_+$ and $\bar{C}_-$ given by Eqs. (16) are uniformly valid for the entire range of ζ from $\zeta = 1$ to $\zeta = 0$. Therefore, it is permissible to evaluate the equations for C_{+1} and C_{-1} at $\zeta = 0$. However, if terms of higher order in ϵ are desired, then the expansions given by Eqs. (14) must be supplemented by "outer" expansions valid for $\zeta = 0(\epsilon)$.

Table 1 Probe characteristic data; adiabatic probe

	K										
r_p*	10^{-30}	10^{-20}	10^{-10}	10^{-5}	10^{-2}	2×10^{-2}	5×10^{-2}	10^{-1}	2×10^{-1}	5×10^{-1}	9×10^{-1}
1000	β_∞ = 491.54 $-\phi_p^*$ = 77.04 $-E_p^*$ = 5.9205	493.58 53.88 5.1371	496.05 30.61 4.0093	497.66 18.82 3.0813	498.98 11.32 2.0238	499.15 10.41 1.8435	499.40 8.993 1.5546	499.59 7.633 1.2848	499.77 5.878 0.95947	499.95 2.791 0.43984	499.99 0.4351 0.067911
100	42.643 74.68 6.4327	44.247 51.43 5.4779	46.332 28.28 4.1802	47.773 16.51 3.1675	49.021 9.073 2.0589	49.186 8.207 1.8734	49.421 6.917 1.5777	49.603 5.758 1.3026	49.778 4.353 0.97191	49.953 2.029 0.44521	49.999 0.3148 0.068727
10	1.8480 72.18 12.074	2.2037 49.05 9.1783	2.8529 25.86 5.9861	3.4989 14.15 4.0578	4.2615 6.857 2.4149	4.3788 6.052 2.1762	4.5508 4.911 1.8099	4.6894 3.962 1.4814	4.8251 2.904 1.0970	4.9629 1.311 0.49918	4.9991 0.2019 0.076933
1	0.038295 70.11 73.408	0.051885 47.00 49.814	0.087102 23.84 25.982	0.14526 12.21 13.828	0.27555 5.143 6.2069	0.30453 4.415 5.3855	0.35170 3.436 4.2561	0.39384 2.677 3.3555	0.43829 1.896 2.4034	0.48652 0.8274 1.0604	0.49967 0.1262 0.16220
0.1	0.0016341 69.20 693.61	0.0024036 46.15 462.90	0.0046714 23.10 232.02	0.0091222 11.57 116.42	0.021774 4.645 46.893	0.025026 3.948 39.891	0.030605 3.027 30.616	0.035852 2.329 23.577	0.041626 1.629 16.511	0.048138 0.7024 7.1255	0.049955 0.1068 1.0836
0.01	0.00014556 69.08 6908.9	0.00021812 46.05 4606.1	0.00043562 23.02 2303.2	0.00087028 11.51 1151.7	0.0021303 4.606 460.82	0.0024577 3.913 391.48	0.0030217 2.996 299.81	0.0035545 2.303 230.45	0.0041430 1.610 161.09	0.0048091 0.6934 69.383	0.0049953 0.1054 10.546

is obtained we shall consider the constant electron temperature case for which $\bar{T}_- = 1$, $\bar{D}_- = \bar{T}_+$, $\bar{D}_+ = \bar{T}_+^{3/2}$, and $\bar{T}_+ = [1 + a/(r_p^* + s)]^{2/3}$ where $a \equiv r_p^*(\bar{T}_p^{3/2} - 1)$. We shall also take τ the ratio of electron to ion temperature at infinity equal to unity. Then by combining Eqs. (6b) and (6c) to eliminate E^*, and introducing the new variables

$$\bar{\beta} = (\beta_+ + \beta_-)/2, \ \delta = (\beta_+ - \beta_-)/2$$

we obtain the following equation:

$$[\bar{T}_+/(\bar{\beta} + \delta)][d(\bar{\beta} + \delta)/ds] + [1/(\bar{\beta} - \delta)][d(\bar{\beta} - \delta)/ds] = [r_p^{*2}/(1 + K)(r_p^* + s)^2]\{[\bar{T}_+^{1/2}/(\bar{\beta} + \delta)] + [K/(\bar{\beta} - \delta)]\} \tag{23}$$

For $s \to \infty$, $\beta_+ \to \beta_-$ and thus $\delta \to 0$. Therefore, for large s we can set $\delta = 0$ in Eq. (23) and we obtain the following equation for determining the asymptotic behavior of $\bar{\beta}$:

$$(1 + \bar{T}_+)(d\bar{\beta}/ds) = (\bar{T}_+^{1/2} + K)r_p^{*2}/(1 + K)(r_p^* + s)^2 \tag{24}$$

On integrating Eq. (24) and making use of the boundary condition $\bar{\beta} = \beta_\infty$ at $s = \infty$ we obtain

$$\bar{\beta} \sim \beta_\infty - [3r_p^{*2}/2a(1 + K)][\xi^2 - \log(1 + \xi^2) + 2K\xi - 2K \tan^{-1}\xi - 2K(1 - \pi/4) - 1 + \log 2] \tag{25}$$

as $s \to \infty$, where $\xi = [1 + a/(r_p^* + s)]^{1/3} = \bar{T}_+^{1/2}$. Similarly, to obtain the asymptotic behavior of the electric field we again combine Eqs. (6b) and (6c) to obtain the following:

$$2\bar{T}_+(d\delta/ds) = [r_p^{*2}\bar{T}_+^{1/2}/(1 + K)(r_p^* + s)^2](1 - K\bar{T}_+^{1/2}) + [(\bar{\beta} + \delta) + \bar{T}_+(\bar{\beta} - \delta)]E^* \tag{26}$$

Again, letting $\delta \to 0$ we obtain

$$E^* \sim \frac{-\bar{T}_+^{1/2}(1 - K\bar{T}_+^{1/2})r_p^{*2}}{\bar{\beta}(1 + K)(1 + \bar{T}_+)(r_p^* + s)^2} \tag{27}$$

as $s \to \infty$, where $\bar{\beta}$ is given by Eq. (25). The corresponding results for the case $\bar{T}_- = \bar{T}_+$ are:

$$\bar{\beta} \sim \beta_\infty + (3r_p^{*2}/4a)(\xi^2 - 1) \tag{28}$$

$$E^* \sim -\frac{1}{2}\frac{(1 - K)}{(1 + K)}\frac{r_p^{*2}\bar{T}^{1/2}}{\bar{\beta}(r_p^* + s)^2} \tag{29}$$

6. Method of Solution and Results

Numerical solutions of Eqs. (6) have been obtained for a wide range of values of r_p^* and K for both the case where the negative-particle temperature is constant but the positive-particle temperature is in equilibrium with the neutral temperature and the case of equal positive- and negative-particle temperatures. All of those results are for a probe temperature ratio $\bar{T}_p = 0.2$ and for $\tau = 1$. In addition, the variation of floating-potential with ratio of probe radius to Debye

Table 2 Probe characteristic data; cold probe (T_p/T_∞ = 0.2) with electrons at local thermal equilibrium

	K										
r_p*	10^{-30}	10^{-20}	10^{-10}	10^{-5}	10^{-2}	2×10^{-2}	5×10^{-2}	10^{-1}	2×10^{-1}	5×10^{-1}	9×10^{-1}
1000	β_∞ = 653.91 $-\phi_p^*$ = 14.66 $-E_p^*$ = 7.7250	655.14 11.86 3.9138	656.61 7.134 3.0587	657.56 4.749 2.3527	658.34 3.216 1.5462	658.44 3.013 1.4085	658.59 2.673 1.1880	658.70 2.316 0.98187	658.80 1.818 0.73324	658.91 0.8790 0.33615	658.94 0.1377 0.051901
100	60.911 17.92 7.9336	62.115 12.38 4.0406	63.574 7.041 3.1225	64.518 4.434 2.3852	65.300 2.807 1.5599	65.401 2.603 1.4203	65.543 2.277 1.1971	65.654 1.951 0.98897	65.760 1.517 0.73825	65.866 0.7263 0.33833	65.893 0.1135 0.052234
10	3.0995 28.60 12.643	3.6625 18.48 5.5762	4.5719 9.161 3.8473	5.3172 4.972 2.7387	6.0217 2.617 1.7036	6.1174 2.360 1.5431	6.2530 1.982 1.2921	6.3594 1.646 1.0626	6.4611 1.242 0.79009	6.5624 0.5781 0.36083	6.5887 0.08966 0.055660
1	0.061487 37.73 73.453	0.083458 25.22 27.495	0.13941 12.74 14.499	0.22717 6.537 7.8783	0.40142 2.800 3.6735	0.43691 2.414 3.2074	0.49292 1.892 2.5573	0.54145 1.483 2.0299	0.59138 1.057 1.4631	0.64434 0.4646 0.64942	0.65859 0.07100 0.099480
0.1	0.0028454 38.36 693.57	0.0041621 25.71 258.08	0.0079230 13.05 131.18	0.014828 6.688 67.384	0.032074 2.797 28.276	0.036170 2.393 24.207	0.043020 1.851 18.739	0.049321 1.433 14.520	0.056143 1.009 10.223	0.063738 0.4370 4.4327	0.065842 0.06653 0.67471
0.01	0.00025972 38.36 6908.5	0.00038569 25.71 2571.1	0.00075049 13.04 1304.7	0.0014301 6.685 668.66	0.0031540 2.794 279.45	0.0035668 2.390 239.05	0.0042596 1.847 184.82	0.0048991 1.430 143.06	0.0055935 1.006 100.61	0.0063689 0.4356 43.576	0.0065841 0.066297 6.6328

Table 3 Cold probe ($T_p/T_\infty = 0.2$) with electrons frozen at T_∞, $K < 1$

	K										
r_p*	10^{-30}	10^{-20}	10^{-10}	10^{-5}	10^{-2}	2×10^{-1}	5×10^{-2}	10^{-1}	2×10^{-1}	5×10^{-1}	9×10^{-1}
1000	β_∞ = 471.36	472.57	474.03	474.96	477.15	478.64	482.78	489.06	499.98	523.89	543.98
	$-\phi_p$* = 75.05	51.88	28.60	16.81	9.325	8.427	7.088	5.892	4.489	2.459	1.212
	$-E_p$* = 7.7250	6.7314	5.2964	4.1149	2.7656	2.5389	2.1841	1.8649	1.4970	0.94394	0.56673
100	42.491	43.725	45.227	46.197	47.715	47.318	47.920	48.647	49.833	52.385	54.375
	74.13	50.94	27.67	15.85	8.347	7.495	6.194	5.130	3.849	2.080	1.003
	7.9336	6.8548	5.3487	4.1396	2.7778	2.5499	2.1931	1.8719	1.5017	0.94494	0.56527
10	1.8999	2.2632	2.9070	3.5106	4.1755	4.2825	4.4549	4.6210	4.8298	5.1774	5.4220
	72.22	49.10	25.92	14.22	6.914	6.104	4.962	4.005	2.983	1.573	0.7157
	12.643	9.7764	6.6084	4.6688	2.9535	2.6966	2.3028	1.9537	1.5547	0.95847	0.55359
1	0.038212	0.051670	0.086204	0.14206	0.26367	0.29110	0.33734	0.38153	0.43352	0.50640	0.54522
	70.11	47.00	23.83	12.19	5.105	4.367	3.392	2.648	1.906	0.9552	0.3846
	73.453	49.861	26.030	13.868	6.2278	5.4115	4.3036	3.4411	2.5592	1.3812	0.63878
0.1	0.0016263	0.0023867	0.0046081	0.0088906	0.020757	0.023852	0.029344	0.034839	0.041486	0.050720	0.055198
	69.20	46.15	23.09	11.54	4.584	3.885	2.968	2.286	1.624	0.7984	0.3054
	693.57	462.82	231.86	116.12	46.250	39.224	29.999	23.137	16.470	8.1290	3.1386
0.01	0.00014493	0.00021671	0.00043010	0.00084922	0.0020337	0.0023458	0.0029016	0.0034595	0.0041356	0.0050741	0.0055259
	69.08	46.05	23.02	11.49	4.548	3.852	2.940	2.263	1.607	0.7891	0.3009
	6908.5	4605.5	2301.9	1149.1	454.94	385.36	294.14	226.43	160.81	78.960	30.114

length has been determined for a range of $\bar{T}_p$ from 0.2 to 1.0 for the case of equal positive- and negative-particle temperatures. The floating potential depends on the ratio $\alpha = D_+/D_-$ which was taken to be equal to 0.00426. This value of α was determined by making the very crude approximation that the ratio of diffusion coefficients is proportional to the square root of the molecular weight ratio, and applying that assumption to the case where the charged particles consist of electrons and NO^+.

The integration is started at the probe surface ($s = 0$) with an assumed value of E_p*. If the assumed value is the correct one for the particular value of K and r_p* chosen, then the value of β_∞ comput'd from the asymptotic formula Eq. (25) or (28) will approach a constant as s becomes large. Also the numerically computed values of E* will agree with the asymptotic values as given by Eq. (27) or (29). The numerical technique consists basically of bracketing the correct value of E_p* and using the method of regula falsi to converge on the proper value that satisfies the asymptotic conditions as described above. The number of significant figures required of E_p* in order to extend the numerical solution into the region where the asymptotic formulas are valid can be as large as 12, depending on r_p* and K.

Once the proper value of E_p* has been determined, the probe potential

$$\phi_p^* = -\int_\infty^0 E^* \, ds$$

can be found.

The results of the numerical computations are given in Tables 1–4. For comparison the results for the uniform temperature case given in Ref. (1) are also included. In order to convert the parameters β_∞, K, and r_p* given in the tables into other quantities of physical interest, the following relations are useful: $\rho_p^2 = N_\infty e^2 r_p^2/\epsilon_0 k T_{-\infty} = \beta_\infty r_p^{*2} = r_p^2/\lambda_D^2$ (dimensionless ambient negative or positive species concentration), $J_+\rho_p^2 = -\Gamma_{+p} e^2 r_p^3/\epsilon_0 k T_{-\infty} D_{+\infty} = r_p^{*3}/(1 + K)$ (dimensionless positive charged particle flux), $J_-\rho_p^2 = -\Gamma_{-p} e^2 r_p^3/\epsilon_0 k T_{-\infty} D_{-\infty} = r_p^{*3} K/(1 + K)$ (dimensionless negative charged particle flux), $J_T = -(\Gamma_{+p} - \Gamma_{-p}) e^2 r_p^3/\epsilon_0 k T_{-\infty} D_{+\infty} = [(1 - K/\alpha)/(1 + K)] r_p^{*3}$ (dimensionless net charge flux, where $\alpha = D_+/D_-$). Because of the symmetry of Eqs. (6) when $\tau = 1$ and $\bar{T}_+ = \bar{T}_-$, it is only necessary to do the numerical computations for $K \leq 1$ for those cases. This is because the results obtained for $K = a_1$, $E_p^* = a_2$, $\phi_p^* = a_3$, $\beta_\infty = a_4$, and $r_p^* = a_5$ can be mapped into $K = 1/a_1$, $E_p^* = -a_2$, $\phi_p^* = -a_3$, $\beta_\infty = a_4$, $r_p^* = a_5$. For $\tau \neq 1$ or for $\bar{T}_+ \neq \bar{T}_-$ the symmetry is destroyed and separate computations must be made for K less than unity and for K greater than unity. Probe characteristics can be constructed from these data for any specified value of α (the ratio $D_{+\infty}/D_{-\infty}$). Typical characteristics for $\alpha = 0.001$ are presented in Fig. 1. Gaps are left in the curves where the data are not spaced closely enough for good resolution. In that figure, ρ_p^2 is the dimensionless charged particle number density in the form $(r_p/\lambda_D)^2$. The characteristics presented therefore span the range of very thin to very thick sheath compared to the probe radius. Agreement of the computed characteristic data with

Table 4 Cold probe ($T_p/T_\infty = 0.2$) with electrons frozen at T_∞, $K > 1$

	K										
r_p*	10^{30}	10^{20}	10^{10}	10^{5}	10^{2}	50	20	10	5	2	1.111111
1000	β_∞ = 616.46	617.18	618.04	618.57	617.55	616.20	612.26	606.12	595.34	571.55	551.50
	$+\phi_p$* = 15.97	11.26	6.545	4.151	2.606	2.406	2.070	1.718	1.215	0.1644	−0.8068
	$+E_p$ = 5.6672	4.8518	3.6419	2.6196	1.4927	1.3101	1.0223	0.75712	0.43990	−0.06586	−0.43156
100	59.054	59.836	60.756	61.317	61.579	61.485	61.143	60.566	59.517	57.155	55.137
	17.21	11.85	6.641	4.069	2.458	2.256	1.922	1.595	1.132	0.1947	−0.6547
	5.7961	4.9422	3.6940	2.6512	1.5094	1.3250	1.0346	0.76730	0.44784	−0.061216	−0.42923
10	3.3278	3.9201	4.8087	5.4491	5.9258	5.9670	5.9997	5.9899	59.253	5.7164	5.5069
	27.65	17.78	8.799	4.798	2.530	2.282	1.900	1.548	1.101	0.2728	−0.4291
	7.7338	6.1747	4.3112	2.9940	1.6792	1.4752	1.1577	0.86852	0.52572	−0.017104	−0.40873
1	0.062807	0.085892	0.14613	0.24360	0.42482	0.45658	0.50200	0.53570	0.56264	0.57243	0.55570
	37.70	25.19	12.72	6.531	2.821	2.434	1.903	1.475	1.011	0.3165	−0.1907
	40.460	27.589	14.630	8.0346	3.7529	3.2551	2.5451	1.9529	1.2976	0.31644	−0.37930
0.1	0.0028712	0.0042168	0.0081195	0.015494	0.033622	0.037569	0.043750	0.048900	0.053713	0.057194	0.056234
	38.36	25.71	13.06	6.713	2.829	2.421	1.864	1.426	0.9670	0.3155	−0.1362
	384.83	258.16	131.34	67.674	28.630	24.503	18.878	14.439	9.7792	3.1618	−1.4230
0.01	0.00026179	0.00039024	0.00076769	0.0014909	0.0032993	0.0036979	0.0043259	0.0048529	0.0053498	0.0057184	0.0056291
	38.36	25.71	13.06	6.710	2.825	2.416	1.860	1.422	0.9636	0.3152	−0.1331
	3836.6	2571.7	1306.0	671.18	282.64	241.71	186.05	142.24	93.397	31.521	−0.13334

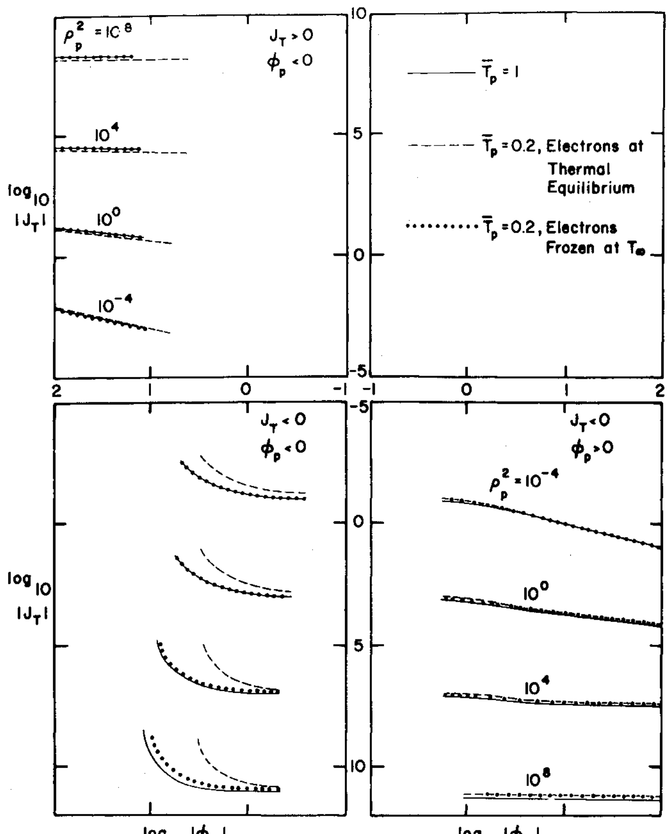

Fig. 1 Probe current-voltage characteristics, $\alpha = 0.001$.

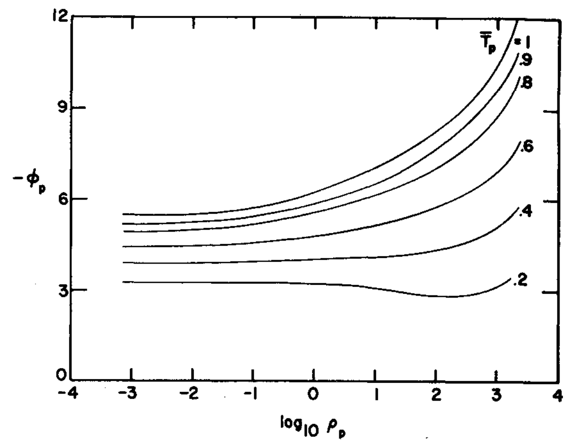

Fig. 2 Floating potential, electrons at thermal equilibrium $\alpha = 0.00426$.

the thin sheath saturation limits and with the point probe solution in the thick sheath limit is excellent. The thin sheath saturation current for the equilibrium electron temperature case is 23% smaller than in the case of an adiabatic probe. For the frozen electron temperature case, it is 6% larger and 19% smaller for saturation on the ion collection and electron collection sides, respectively. The magnitude of these effects is quite small in view of other larger uncertainties in the interpretation of electrostatic probe experiments. Significant effects occur only at small bias potentials for the case in which the electrons are at thermal equilibrium. This can also be seen in Fig. 2 which presents the floating (zero current) potential for the case in which $\alpha = 0.00426$. The floating potential becomes smaller in magnitude and less sensitive to the charged particle number density as the probe is cooled.

7. Conclusions

The idealized problem of a cooled spherical electrostatic probe in a quiescent continuum slightly ionized chemically frozen gas has been investigated. The electron temperature is described by two limiting models; either the electrons are assumed to be at local thermal equilibrium, or they are assumed frozen at the ambient temperature far from the probe. From numerical solutions of the governing equations, it has been found that with the frozen electron temperature assumption, the probe characteristics for a cold probe are only slightly altered from those of an adiabatic probe. With the electrons at thermal equilibrium, the probe characteristic is only slightly altered when the bias potential is large, but significant changes in the probe characteristic do occur when the bias potential is small, including a significant shift in the floating potential.

References

[1] Cohen, I. M., "Asymptotic Theory of Spherical Electrostatic Probes in a Slightly Ionized, Collision-Dominated Gas," *The Physics of Fluids*, Vol. 6, No. 10, Oct. 1963, pp. 1492–1499.

[2] Su, C. H. and Lam, S. H., "Continuum Theory of Spherical Electrostatic Probes," *The Physics of Fluids*, Vol. 6, No. 10, Oct. 1963, pp. 1479–1491.

[3] Cicerone, R. J. and Bowhill, S. A., "Positive Ion Collection by a Spherical Probe in a Collision-Dominated Plasma," Rept. AR-21, 1967, Aeronomy Lab., Dept. of Electrical Engineering, Univ. of Illinois, Urbana, Ill.

[4] Radbill, J. R., "Computation of Electrostatic Probe Characteristics by Quasilinearization," *AIAA Journal*, Vol. 4, No. 7, July 1966, pp. 1195–1200.

[5] Baum, E. and Chapkis, R. L., "Theory of a Spherical Electrostatic Probe in a Continuum Gas: An Exact Solution," *AIAA Journal*, Vol. 8, No. 6, June 1970, pp. 1073–1077.

[6] Thomas, D. L., "Continuum Theory of Cooled Spherical Electrostatic Probes," *The Physics of Fluids*, Vol. 12, No. 2, Feb. 1969, pp. 356–360.